Two Competitive Routes in the Lactim−Lactam Phototautomerization of a Hydroxypyridine Derivative Cation in Water: Dissociative Mechanism versus Water-Assisted Proton Transfer

J. Carlos Penedo,[‡] M. Carmen Ríos Rodríguez, Iria García Lema, J. Luis Pérez Lustres,[§] Manuel Mosquera,* and Flor Rodríguez-Prieto*

Departamento de Química Física, Facultade de Química, Universidade de Santiago de Compostela, E-15782 Santiago de Compostela, Spain

Received: April 8, 2005; In Final Form: September 2, 2005

Ground-state tautomerism and excited-state proton-transfer processes of 2-(6′-hydroxy-2′-pyridyl)benzimidazolium in H_2O and D_2O have been studied by means of UV−vis absorption and fluorescence spectroscopy in both steady-state and time-resolved modes. In the ground state, this compound shows a tautomeric equilibrium between the lactim cation, protonated at the benzimidazole N(3), and its lactam tautomer, obtained by proton translocation from the hydroxyl group to the pyridine nitrogen. Direct excitation of the lactam tautomer leads to its own fluorescence emission, while as a result of the increase of acidity of the OH group and basicity at the pyridine N upon excitation, the lactim species undergoes a proton translocation from the hydroxyl group to the nitrogen, favoring the lactam structure in the excited state. No fluorescence emission from the initially excited lactim species was detected due to the ultrafast rate of the excited-state proton-transfer processes. The lactim−lactam phototaumerization process takes place via two competitive excited-state proton-transfer routes: a one-step water-assisted proton translocation (probably a double proton transfer) and a two-step pathway which involves first the dissociation of the lactim cation to form an emissive intermediate zwitterionic species and then the acid-catalyzed protonation at the pyridine nitrogen to give rise to the lactam tautomer.

Introduction

Photoinduced excited-state proton-transfer reactions are involved in many chemical and biological areas. Since the initial works of Förster and Weller,[1−3] many research efforts have been focused on the understanding of the dynamics of excited-state proton-transfer reactions in bulk solvents, isolated molecules and clusters, continuing this topical issue as a very active area of research owing to unravel the complex molecular mechanism of these processes.[4−13] Among these reactions, the photoinduced transfer of a proton between an acid and a basic site in a bifunctional molecule is an active topic that has received considerable attention.[3−5,7−13] In these species, both proton donor and acceptor groups may undergo a simultaneous increase of acidity and basicity upon electronic excitation, providing the driving force for migration of the proton from the acid to the basic site and leading to a phototautomer. Depending on the relative position of the donor and acceptor groups within the molecule and the nature of the surrounding molecules, the phototautomerization can take place in three distinct ways: (a) intramolecularly, via a pre-established hydrogen bond between the acid and basic sites (excited-state intramolecular proton transfer or ESIPT), (b) stepwise, facilitated by the solvent, with protonation and deprotonation consecutive reactions through an intermediate species, and (c) double- or multiple-proton transfer (sequential or concerted) in a hydrogen-bond network linking the donor and the acceptor through one or more bifunctional molecules with hydrogen bonding accepting and donating abilities, acting as bridge between the donor and the acceptor sites.

An appealing bifunctional molecule is 2-hydroxypyridine (lactim form), which depending on solvent and other conditions experiences a proton translocation from the hydroxyl group to the pyridine nitrogen, forming 2-pyridone (lactam tautomer). The factors influencing the tautomeric equilibrium in ground and excited states and the interconversion mechanism have received considerable attention from experimental and theoretical points of view.[14−30] The geometry of the molecule does not facilitate the intramolecular proton transfer, and the tautomerization has been shown to take place by double proton transfer in bridged hydrogen-bonding dimers or complexes with other bifunctional molecules (water, alcohol, ...). Other examples of much studied bifunctional molecules which show photoinduced double proton-transfer processes are 7-azaindole, 1-azacarbazole, hydroxyquinolines, pyridylindoles, and related structures.[4,5,8,9,13]

The properties of H-bonding complexes of bifunctional molecules such as 2-pyridone and other heterocycles have attracted a great deal of attention not only due to its intrinsic interest but also for other reasons. First of all, H-bonding complexes show similarities with nucleic acid base pairs and have been proposed as base-pairs analogues to study some of their properties (uracil and thymine show the same H-bonding sites as 2-pyridone).[8,18,31,32] One of the matters of interest is the photoinduced proton-transfer processes in the H-bonding complexes, that have been hypothesized as a possible source of photoinduced mutagenesis.[31−36] Interestingly, an excited-state proton-transfer process in nucleic acid base pairs has been

* To whom correspondence should be addressed. E-mail: (F.R.-P.) qfflorrp@usc.es; (M.M.) qfmmgfot@usc.es.

‡ Current address: Cancer Research UK, Dundee University, Dundee, U.K.

§ Current address: Institut für Chemie, Humboldt University, Berlin, Germany.

10.1021/jp0518355 CCC: $30.25
Published on Web 10/26/2005

CHART 1: Molecular Structures of the Lactim and Lactam Neutral Tautomers and Three Possible Monocations of Species 1

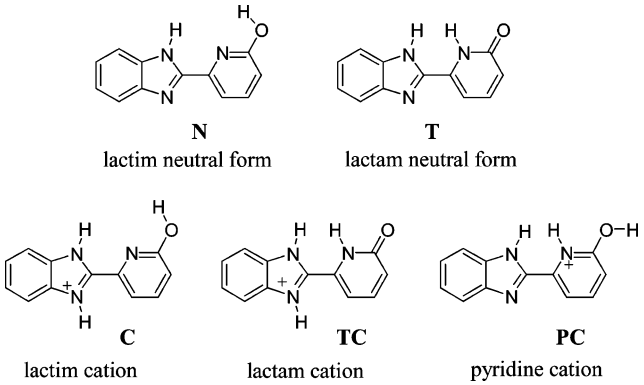

recently proposed as an important mechanism behind the high photostability of DNA base pairs.[37,38] Moreover, the lactam ring appears in many molecules of biological relevance, from nucleotide bases (uracil, thymine, cytosine, and guanine) to antibiotics and proteins (for example, it appears in the chromophore of the green fluorescent protein). Hydrogen bonding and proton transfer are usually key features in the reactivity of these molecules, for example in the aminolysis of β-lactam antibiotics, which was shown to be catalyzed by H-bonding bifunctional molecules.[39] In a rather different field, an anhydrous proton conductor based on lactam−lactim tautomerism of uracil has been recently presented.[40] It has been suggested a Grotthuss-type proton-hopping mechanism for this proton conductor, which could be useful for polymer electrolyte membrane fuel cells.

Some time ago we began an extensive research into the photophysics of a derivative of 2-hydroxypyridine developed in our group, 2-(6′-hydroxy-2′-pyridyl)benzimidazole (**1**, see Chart 1).[41−43] In similar molecules with the hydroxyl group in the ortho position with respect to the benzimidazole moiety, an ESIPT process takes place from the hydroxyl group to the benzimidazole N(3) via a ground-state pre-established hydrogen bond.[44−46] The meta position of the hydroxyl group in **1** precludes the possibility of ESIPT but opens new ways with regard to its tautomeric reactions, with two acid and two basic sites and the possibility to form hydrogen-bond networks. We studied the rich and complex behavior of **1** in acetonitrile, ethanol, and water[41] and showed that there is an equilibrium in the ground state between the lactim form (**N**) and the lactam tautomeric form (**T**) (see Chart 1), favoring the latter as the solvent polarity is increased. In protic solvents, the excitation of the neutral form **N** yields a phototautomer whose nature is different depending on the solvent. In water, the proton migrates from the hydroxyl group to the pyridine nitrogen, whereas in ethanol this translocation takes place from the N−H benzimidazole to the pyridine nitrogen. The latter process was also detected for the anionic form of **1** in basified ethanol and water[42] and for various related structures in alcohols and water.[5,9,47−49] All these proton-transfer processes are assisted by the solvent, and we showed for the phototautomerization of the anion in ethanol at low temperatures that the process is controlled by the solvent reorganization.[42]

We studied also the behavior of **1** in acidified acetonitrile,[43] showing that the lactim cation (**C**), protonated at the benzimidazole N(3), see Chart 1, is the species present in the ground state and does not tautomerize in the excited state. However, in the presence of small amounts of alcohols, **C*** experiences an alcohol-assisted phototautomerization from the OH group to the pyridine N, giving the tautomeric lactam cation **TC***. The formation of this tautomeric cation occurs mainly via a cyclical complex between the cation **C*** and two molecules of alcohol, although it has been observed that a small fraction of **C*** also forms a suitable precursor of **TC*** with just one alcohol molecule. The mechanism of phototautomerization of the related cation 2-(3′-hydroxy-2′-pyridyl)benzimidazolium was also investigated, showing a complex solvent-dependent behavior.[50] In acetonitrile, it does not tautomerize, in ethanol it deprotonates to form a neutral keto species, and in water it undergoes a two-step tautomerization by two different protonation−deprotonation routes.

In this paper we present an extensive study concerning the excited-state proton-transfer mechanism of **1** in acidified H_2O and D_2O. The combined application of steady-state, time-resolved fluorescence, and principal component global analysis allowed us to establish the details of the kinetic mechanism and the rate constants involved.

Experimental Section

Compound **1** was prepared and purified as described elsewhere.[43] Solutions were made up in double-distilled water treated with $KMnO_4$, spectroscopy grade acetonitrile (Scharlau), and D_2O from Sigma (99.9% D) and were not degassed. Acidity was varied with $HClO_4$. pH_c was calculated as $-\log([H^+]/\text{mol dm}^{-3})$. All experiments were carried out at 25 °C.

UV−vis absorption spectra were recorded in a Varian Cary 3E spectrophotometer. Fluorescence excitation and emission spectra were recorded in a Spex Fluorolog-2 FL340 E1 T1 spectrofluorometer, with correction for instrumental factors by means of a Rhodamine B quantum counter and correction files supplied by the manufacturer. Fluorescence lifetimes were determined by single-photon timing in an Edinburgh Instruments FL-900 spectrometer equipped with a hydrogen-filled nanosecond flash lamp and the reconvolution analysis software supplied by the manufacturer. This procedure involves convoluting a theoretical model representing the kinetics of the measured data with an instrument response function and then comparing this to the measured decay data.

Theoretical equations were fitted to the experimental data by means of a nonlinear weighted least-squares routine based on the Marquardt algorithm. Principal component global analyses were performed with Matlab 6.0 for Windows.

Results

1. Absorption Spectra. The absorption spectra of **1** were recorded in aqueous solution over the pH_c range 5.00−1.96 (Figure 1a). The spectrum shifted to the blue on going from neutral to acidic aqueous solution and isosbestic points appeared around 30 000, 37 000, and 41 000 cm^{-1}. The spectrum obtained in the most acid solution showed an intense band with maximum at 31 200 cm^{-1} (band I) and a weak band around 28 000 cm^{-1} (band II). The absorption spectrum of **1** in acidified acetonitrile (Figure 1b) showed only one band located at the same position as that of band I in water. The spectra of **1** in D_2O were similar to H_2O (results not shown).

2. Fluorescence Spectra and Lifetimes. The fluorescence spectra of **1** over a wide range of acidity were recorded in both H_2O and D_2O under excitation at absorption bands I and II. As the spectra obtained in both solvents were very alike, only the results in water are shown in Figure 2.

Under excitation at 28 570 cm^{-1} (band II), the emission band was located at 25 000 cm^{-1} at pH_c 4.10 (Figure 2a). As the acidity increased, the maximum of this band shifted to the red (23 500 cm^{-1} at pH_c 1.54), and its intensity increased by a factor

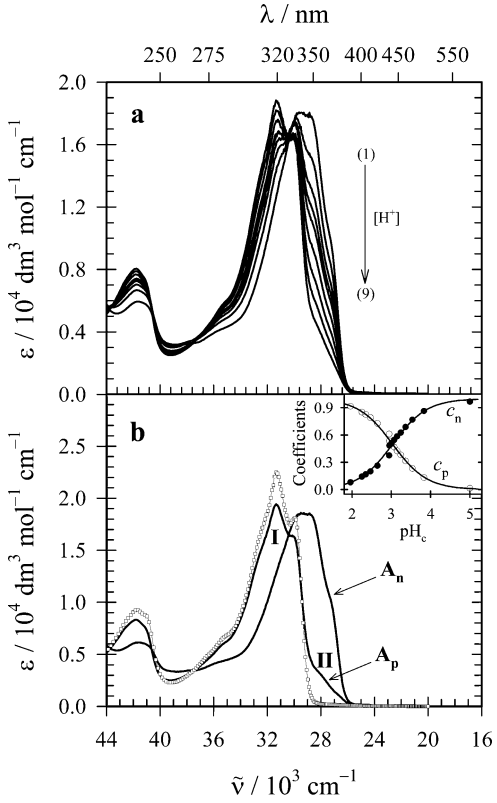

Figure 1. (a) Absorption spectra of **1** in aqueous solution at various pH_c values from 5.00 (1) to 1.96 (9). (b) Absorption spectrum of **1** in acidified acetonitrile (−□−, $[HClO_4] = 3.4 \times 10^{-3}$ mol dm^{-3}), together with the absorption spectra of the neutral ($\mathbf{A}_n$) and the protonated ($\mathbf{A}_p$, showing bands I and II) forms of **1**, obtained applying principal component global analysis to a series of 15 absorption spectra, some of which are plotted in part (a). The inset shows the coefficients representing the contributions of these spectra to the experimental absorption spectra at each acidity. Molar absorption coefficients ϵ are global values, calculated as the quotient of absorbance divided by the absorption path length and the total concentration of **1**. $[\mathbf{1}] = 1 \times 10^{-4}$ mol dm^{-3}.

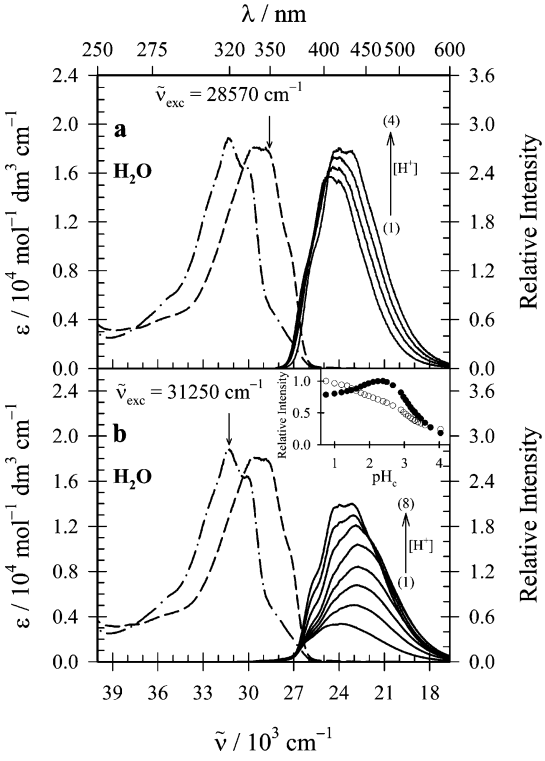

Figure 2. (a) Fluorescence spectra of **1** in aqueous solution under excitation at band II ($\tilde{\nu}_{exc} = 28\,570$ cm^{-1}) with pH_c values in the range 4.10 (1)−1.54 (4), together with the absorption spectra at $pH_c = 5.00$ (− − −) and $pH_c = 1.96$ (−•−•−). (b) Fluorescence spectra of **1** in aqueous solution excitation at band I ($\tilde{\nu}_{exc} = 31\,250$ cm^{-1}) with decreasing pH_c in the range 4.03 (1)−0.75 (8), together with the absorption spectra at $pH_c = 5.00$ (− − −) and $pH_c = 1.96$ (−•−•−). The inset shows the dependence on acidity of the fluorescence intensity at $\tilde{\nu}_{em} = 24\,010$ cm^{-1} (○) and at 20 000 cm^{-1} (●), normalized at the maximum intensity in the range. $[\mathbf{1}] = 3 \times 10^{-6}$ mol dm^{-3}.

of 1.2. When the excitation was performed at 31 250 cm^{-1}, maximum of absorption band I, the fluorescence spectra obtained at pH_c 4 and pH_c below 1.5 (Figure 2b) were similar to those obtained at the same acidity under excitation in band II. However, at intermediate pH_c values the emission behavior was remarkably different. Thus, as the pH_c decreased from 4 to 2, the emission band (peaking at ∼25 000 cm^{-1}) shifted to the red (maximum at ∼22 800 cm^{-1}), and an isoemissive point was detected at 26 500 cm^{-1}. Further increase in the acidity from pH_c 2.00 to pH_c 0.76 shifted the spectrum to the blue until the emission spectrum (peaking at about 24 000 cm^{-1}) matched that obtained under excitation in band II. The emission intensity as a function of pH_c showed also different profiles depending on the monitoring emission wavenumber (inset of Figure 2b): at 24 000 cm^{-1}, the emission intensity increased continuously on decreasing pH_c from 4 to 1, whereas at 20 000 cm^{-1} the intensity showed a maximum at an intermediate acidity around pH_c 2.

Time-resolved fluorescence of **1** in acidic media ($pH_c < 2$) under excitation at absorption band II was independent of pH_c and emission wavenumber and showed monoexponential decay with a lifetime of 2.10 ns in H_2O and 2.37 ns in D_2O. When the excitation was performed at the maximum of absorption band I, the fluorescence decay was biexponential in both solvents at all the wavenumbers studied (23 810 and 21 740 cm^{-1} for H_2O and 25 000, 23 260, and 21 280 cm^{-1} for D_2O), see the Supporting Information. One of the decay times, τ_1, was pH independent, its value matching that obtained exciting at the maximum of absorption band II. On the contrary, the second decay time, τ_2, showed pronounced acidity dependence, its value decreasing as the pH decreased. As both components showed very similar values at high acidity (at approximately $[HClO_4] > 1.5 \times 10^{-2}$ mol dm^3 for H_2O and $[HClO_4] > 2.5 \times 10^{-2}$ mol dm^3 for D_2O), a global analysis of the time-resolved fluorescence data at all the emission wavenumbers studied was performed in both media, keeping fixed the decay time τ_1 with the same value as that obtained under the excitation in band II (2.10 ns in H_2O and 2.37 ns in D_2O). The values of τ_2 and the amplitudes ratio B_1/B_2 obtained in this way are shown in Figures 3 and 4 for H_2O and D_2O, respectively.

Discussion

1. Interpretation of the Absorption Spectra of 1 in Acidic Aqueous Solution: Lactim−Lactam Tautomeric Equilibrium between Cations in the Ground State. The blue shift observed in the absorption spectra as the acidity increased and the isosbestic points detected indicate the existence of an acid−base equilibrium in this acidity range involving the protonation of the neutral forms (equilibrium acidity constant K_a, expressed in terms of concentrations of the species involved). Any absorption spectrum in the acidity range studied, **A** (measured at n_w discrete wavenumbers), must be a combination of the spectra of the neutral forms, $\mathbf{A}_n$, and the protonated forms, $\mathbf{A}_p$, as expressed in eqs 1−3. In these equations, c_n and c_p are the acidity-dependent contributions of the spectra of the neutral

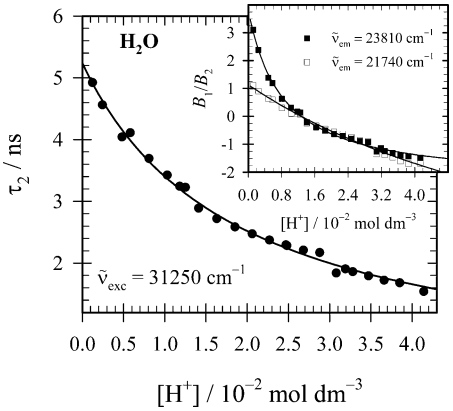

Figure 3. Acidity dependence of the decay time τ_2 obtained from the global biexponential fit of the fluorescence decay of **1** in H_2O at 23 810 cm^{-1} and at 21 740 cm^{-1} ($\tilde{\nu}_{exc} = 31\,250\ cm^{-1}$) with a fixed value of the decay time τ_1 (2.10 ns), together with the fit of eq 14 to τ_2 (solid line). The amplitudes ratio B_1/B_2 provided by this analysis at both emission wavenumbers are shown in the inset together with the fit of eq 15 to these data (solid lines).

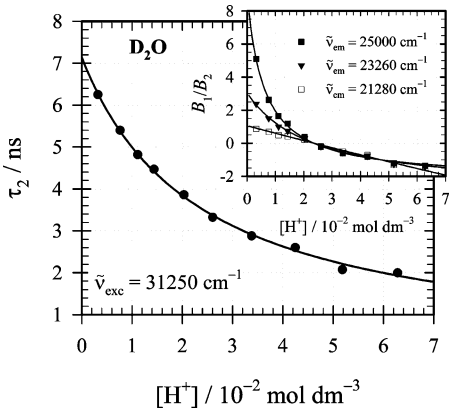

Figure 4. Acidity dependence of the decay time τ_2 obtained from the global biexponential fit of the fluorescence decay of **1** in D_2O at 25 000, 23 260, and 21 280 cm^{-1} ($\tilde{\nu}_{exc} = 31\,250\ cm^{-1}$) with a fixed value of the decay time τ_1 (2.37 ns), together with the fit of eq 14 to τ_2 (solid line). The amplitudes ratio B_1/B_2 provided by this analysis at the monitoring emission wavenumbers are shown in the inset together with the fit of eq 15 to these data (solid lines).

species (**N** and **T**)[41] and the protonated species to the global absorption spectra.

$$\mathbf{A} = c_n\mathbf{A}_n + c_p\mathbf{A}_p \quad (1)$$

$$c_n = \frac{K_a}{K_a + [H^+]} \quad (2)$$

$$c_p = \frac{[H^+]}{K_a + [H^+]} \quad (3)$$

Principal component analysis has proven to be very useful to determine the number of independent "component spectra" linearly contributing to the changes observed in the experimental spectra as a function of a systematically changed variable (acidity in our case).[51,52] Also, when it is combined with the equations derived from a model (like the acid−base equilibrium described by eqs 1−3), it is possible to obtain accurate estimations of the independent component spectra. Principal component analysis was applied to the series of absorption spectra in Figure 1a, and the result showed that two independent components are needed to reproduce all the experimental spectra of the series. A nonlinear global analysis combined with principal component analysis (principal component global analysis)[52] was also carried out to test the model functions describing the acidity dependence of coefficients c_n and c_p (eqs 2 and 3) and to find estimations of K_a and the component spectra $\mathbf{A}_n$ and $\mathbf{A}_p$. In this way, eqs 1−3 were globally fitted to all the spectra at all available wavenumbers simultaneously, yielding the calculated component spectra $\mathbf{A}_n$ and $\mathbf{A}_p$ and the coefficients c_n and c_p plotted in Figure 1b, and the acidity constants shown in Table 1.

The absorption spectrum $\mathbf{A}_p$ of the protonated form of **1** obtained from principal component global analysis (almost coincident with the spectrum recorded experimentally at pH_c 2.0) is very similar to that measured in acidified acetonitrile (Figure 1b), except in the red edge 29 000−26 000 cm^{-1} (band II). The new band II present in water could be due to the existence of two monocations in the ground state. This hypothesis is supported by the different fluorescence behavior observed under excitation at each individual band (see below). We have already shown[41] that in neutral aqueous conditions compound **1** shows a tautomeric equilibrium between the lactim form **N** and the lactam tautomer **T**. From the different protonation sites available in these neutral structures, we can identify three possible monocations (see Chart 1), two resulting from protonation of the lactim form, either at the benzimidazole N(3) (**C**) or at the pyridine nitrogen (**PC**), and one obtained from protonation of the lactam structure at the benzimidazole N(3) (**TC**). It is known that protonation at the benzimidazole N(3) in pyridylbenzimidazoles does not change the absorption spectrum significantly, whereas protonation at the pyridine N induces a red shift in the absorption spectra.[47,50,53,54] Taking into account that the maximum of bands I and II in acidic aqueous solution are very close to those reported previously[41] for the neutral structures **N** (31 700 cm^{-1}) and **T** (29 800 cm^{-1}), we rule out **PC** and suggest **C** (band I) and **TC** (band II) as the monocations responsible for the absorption in acidic aqueous solution. Further evidences are obtained from the similarities in shape and position between band I and the absorption spectrum reported in acidified acetonitrile (Figure 1b), where **C** is the only monocation present in the ground state.[43] Based on these similarities and assuming (a) that the absorption from **TC** is negligible at the absorption maximum of **C** (the almost coincident shape of band I with the spectrum measured in acetonitrile supports this hypothesis) and (b) that the molar absorption coefficient of **C** does not change from acetonitrile

TABLE 1: Acidity Constant K_a, Tautomeric Equilibrium Constant K = [TC]/[C], and Fluorescence Quantum Yields Φ Obtained for the Protonated Forms of 1 in H_2O and D_2O Using Various Approaches

	H_2O			D_2O		
	absorption spectra	fluorescence spectra (excitation at band II)	fluorescence spectra (excitation at band I)	absorption spectra	fluorescence spectra (excitation at band II)	fluorescence spectra (excitation at band I)
pK_a	3.033 ± 0.009	2.975 ± 0.012	3.127 ± 0.004	3.419 ± 0.006	3.532 ± 0.011	3.586 ± 0.007
K	∼0.16			∼0.24		
Φ_{TC}		0.31	0.34		0.36	0.29
Φ_Z			0.38			0.65

to water, the lactim−lactam tautomeric equilibrium constant $K = [\mathbf{TC}]/[\mathbf{C}]$ is estimated to be ~0.16 in H_2O and ~0.24 in D_2O.

To sum up, **1** exists in acidic aqueous solution as two protomeric forms in equilibrium, the lactim cation **C** and the lactam cation **TC**, the latter not detected in acetonitrile.[43] This behavior is consistent with the general trend observed for other hydroxypyridines, the more polar lactam tautomer being favored by increasing the polarity and the hydrogen-bond donating ability of the solvent.[55]

2. Interpretation of the Fluorescence Spectra and Lifetimes of 1 in Acidic Aqueous Solution under Selective Excitation of the Lactam Cation TC at Absorption Band II: Emission from TC*. Selective excitation of the neutral lactam tautomer **T** at wavenumbers below 29 000 cm^{-1} in aqueous solution of pH ~5.00 led to its own fluorescence, with a maximum at 24 440 cm^{-1}.[41] As the pH decreases, **T** protonates at the benzimidazole N(3) to give the lactam cation **TC**, which was the only species contributing to the absorption band II at pH_c values below ~2.00. At this pH_c, upon excitation of **TC**, a fluorescence band with maximum at ~24 000 cm^{-1} in water (Figure 2a) and D_2O was detected. This fluorescence emission overlaps the absorption band II and therefore must be due to **TC***. The fluorescence decay of **TC*** was monoexponential with a lifetime of 2.10 ns in water and 2.37 ns in D_2O. These values did not depend on acidity, indicating that **TC*** does not undergo any pH-dependent excited-state process. The changes observed in the fluorescence spectra on going from neutral to acidic conditions can be completely justified by the pH dependence of the ground-state concentrations of both emitting species **T*** and **TC***. Assuming a linear dependence of the fluorescence intensity with the absorbance ($A < 0.08$ at the excitation wavenumber employed), the $[H^+]$ dependence of the fluorescence spectra under excitation at 28 570 cm^{-1} is easily deduced, leading to eqs 4−6.

$$\mathbf{F} = c_{\mathbf{T}}\mathbf{F}_{\mathbf{T}} + c_{\mathbf{TC}}\mathbf{F}_{\mathbf{TC}} \tag{4}$$

$$c_{\mathbf{T}} = \frac{K_a}{K_a + [H^+]} \tag{5}$$

$$c_{\mathbf{TC}} = \frac{[H^+]}{K_a + [H^+]} \tag{6}$$

In these equations, **F** represents any experimental fluorescence spectrum like those shown in Figure 2a, $\mathbf{F_T}$ and $\mathbf{F_{TC}}$ are the pure fluorescence spectra of **T*** and **TC***, and $c_{\mathbf{T}}$ and $c_{\mathbf{TC}}$ are the coefficients which represent the contributions of **T*** and **TC*** to the experimental spectra at each pH. The application of principal component analysis to a series of 24 fluorescence spectra (some of them plotted in Figure 2a) showed that two independent components are needed to reproduce the experimental spectra. Furthermore, principal component global analysis allows us to calculate the pure fluorescence spectra of **T*** and **TC*** (Figure 5) and their contributions to the experimental spectra at each acidity, $c_{\mathbf{T}}$ and $c_{\mathbf{TC}}$ (see inset in Figure 5). The spectrum of **T*** matches that obtained at neutral pH (square symbols in Figure 5).[41] We obtained from the fit the pK_a values in H_2O and D_2O shown in Table 1, in good agreement with those previously obtained from the absorption data. Finally, from the absorbance values of **T** and **TC** in water at $\tilde{\nu}_{exc} = 28\,570$ cm^{-1}, and knowing the areas of the pure fluorescence spectra of **T*** and **TC*** (Figure 5), the ratio $\Phi_{\mathbf{TC}}/\Phi_{\mathbf{T}}$ was calculated to be 4.78 in water. Taking into account that $\Phi_{\mathbf{T}} = 0.065$,[41] $\Phi_{\mathbf{TC}}$ is estimated to be 0.31 in this solvent. An analogous procedure led to $\Phi_{\mathbf{TC}} = 0.36$ in D_2O.

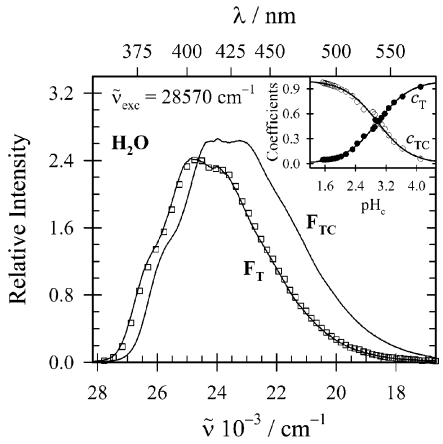

Figure 5. Pure fluorescence spectra (solid lines) of the lactam neutral form **T*** and the lactam cation **TC*** obtained applying principal component global analysis to a series of 24 fluorescence spectra recorded under excitation at band II ($\tilde{\nu}_{exc} = 28\,570$ cm^{-1}) in acid aqueous solution (part of the spectra are plotted in Figure 2a). The square symbols (□) represent the experimental fluorescence spectrum of **1** obtained in neutral aqueous solution under excitation at 28 170 cm^{-1}. The coefficients representing the contributions of the pure fluorescence spectra of **T*** (●) and **TC*** (○) to the experimental spectrum at each pH_c are plotted in the inset together with the fit of eqs 5 and 6 to these coefficients (solid lines).

3. Interpretation of the Fluorescence Spectra of 1 in Acidic Aqueous Solution under Selective Excitation of the Lactim Cation C at Absorption Band I: Emission from the Lactam Cation TC* and the Zwitterion Z*. The behavior of **1** under excitation at band I (31 250 cm^{-1}) is more complicated than that observed at band II. At low acidity, direct excitation of **N** and **T**, which are the only species present in the ground state, leads to their own emission with a certain amount of **T*** formed from **N*** via a proton-transfer process from the hydroxyl group to the pyridine nitrogen.[41] At pH_c ~0.8 only the monocations **C** (the major species) and **TC** are present in the ground state. At the excitation wavenumber employed, **C** is the main absorbing species, but the fluorescence spectrum recorded (Figure 2b) is very similar to the band obtained under excitation at band II. This suggests that the emitting species is **TC*** and therefore the existence of a **C*** → **TC*** process. Further information about the type of process taking place can be gained from the fluorescence changes observed as the acidity is increased. Thus, from pH_c ~4 to pH_c ~2, the fluorescence emission maximum shifts to the red, but from pH_c ~2 to pH_c ~0.8 the emission band shifts to the blue and becomes very similar to that obtained under direct excitation of **TC** at band II. This is clearly shown by the emission-wavelength dependence of the fluorescence intensity-pH_c traces as it is seen in the inset of Figure 2b. Thus, at 24 000 cm^{-1} the fluorescence intensity rises as the pH_c falls, while at 20 000 cm^{-1} the emission intensity increases up to pH_c ~2 and from there decreases. These evidences together with the fact that this behavior is not observed under excitation of **TC** suggest that upon excitation, **C*** undergoes an excited-state process to yield a new species, with emission around 20 000 cm^{-1}. The contribution of the fluorescence from this species reaches a maximum at intermediate acidity and then is quenched by H^+ to give the monocation **TC***. The quenching observed suggests a neutral structure, and we propose here a zwitterion, **Z***, resulting from the deprotonation of **C*** at the hydroxyl group (rate constant k_1, see Scheme 1). This assignment is supported by the behavior observed for

SCHEME 1: Excitation and Deactivation of 1 in Acidic Aqueous Solution

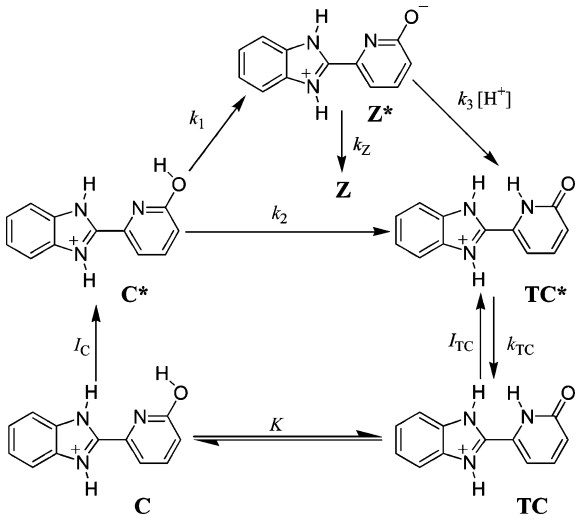

similar monocations, like 2-(3′-hydroxy-2′-pyridyl)benzimidazolium[50] and its 1-methyl derivative[45] and 2-(2′-hydroxyphenyl)-benzimidazolium,[46] which upon excitation dissociate due to the increase of acidity at the hydroxyl group. Once the zwitterion **Z*** is formed, this can either emit or, if the concentration of protons is high enough, protonate at the pyridine nitrogen with rate constant k_3, leading to **TC***.

We have previously reported the formation of **TC*** from **C*** in binary mixtures of acetonitrile with alcohols via an alcohol-assisted proton translocation, and here we suggest that a similar water-assisted phototautomerization **C*** → **TC*** could also take place (rate constant k_2 in Scheme 1). Evidences for the existence of this process will be presented later on in this paper.

The excited-state reactions experienced by **C*** must be ultrafast, as no fluorescence from **C*** was detected (in acetonitrile its fluorescence is strong[43]). We suppose therefore that the rate constants k_1 and k_2 are much greater than the deactivation constant of **C***, which for that reason was not included in Scheme 1. According to the above interpretation, we propose the mechanism of Scheme 1 to explain the behavior of **1** in acidic aqueous solution. In the next sections, more evidences are presented to support this mechanism.

4. Interpretation of the Fluorescence Lifetimes of 1 in Acidic Aqueous Solution under Selective Excitation of the Lactim Cation C at Absorption Band I: C* → TC* Phototautomerization Takes Place via Two Competitive Routes. From the mechanism of Scheme 1, the time dependence of [**Z***] and [**TC***] under selective excitation of **C** at band I are given by eqs 7 and 8. We have taken into account that at time zero in the nanosecond time scale of our experiments **C*** has already disappeared by transformation into **Z*** and **TC***, which will have initial concentrations $[\mathbf{Z^*}]_0$ and $[\mathbf{TC^*}]_0$ according to the values of the ultrafast rate constants k_1 and k_2 and the amount of **C** excited.

$$-\frac{\mathrm{d}[\mathbf{Z^*}]}{\mathrm{d}t} = (k_{\mathbf{Z}} + k_3[\mathrm{H^+}])[\mathbf{Z^*}] \tag{7}$$

$$-\frac{\mathrm{d}[\mathbf{TC^*}]}{\mathrm{d}t} = k_{\mathbf{TC}}[\mathbf{TC^*}] - k_3[\mathrm{H^+}][\mathbf{Z^*}] \tag{8}$$

Considering that at the monitoring emission wavenumbers both **Z*** and **TC*** fluoresce, their fluorescence intensities ($F_{\mathbf{Z}(\tilde{\nu},t)}$ and $F_{\mathbf{TC}(\tilde{\nu},t)}$) and the total fluorescence intensity ($F_{(\tilde{\nu},t)}$) at time t and wavenumber $\tilde{\nu}$, are related to the time-dependent concentrations $[\mathbf{Z^*}]_{(t)}$ and $[\mathbf{TC^*}]_{(t)}$ by eqs 9−11

$$F_{\mathbf{Z}(\tilde{\nu},t)} = \omega_{\mathbf{Z}(\tilde{\nu})}[\mathbf{Z^*}]_{(t)} \tag{9}$$

$$F_{\mathbf{TC}(\tilde{\nu},t)} = \omega_{\mathbf{TC}(\tilde{\nu})}[\mathbf{TC^*}]_{(t)} \tag{10}$$

$$F_{(\tilde{\nu},t)} = F_{\mathbf{Z}(\tilde{\nu},t)} + F_{\mathbf{TC}(\tilde{\nu},t)} \tag{11}$$

where $\omega_{\mathbf{Z}(\tilde{\nu})}$ and $\omega_{\mathbf{TC}(\tilde{\nu})}$ are wavenumber-dependent parameters determined by the fluorescence properties of the respective species and instrumental factors. Integration of eqs 7 and 8 with the above initial conditions allows the time dependence of the total fluorescence to be easily derived (eqs 12−18).

$$F_{(\tilde{\nu},t)} = B_{1(\tilde{\nu})}\exp(-t/\tau_1) + B_{2(\tilde{\nu})}\exp(-t/\tau_2) \tag{12}$$

$$\tau_1^{-1} = k_{\mathbf{TC}} \tag{13}$$

$$\tau_2^{-1} = k_{\mathbf{Z}} + k_3[\mathrm{H^+}] \tag{14}$$

$$\frac{B_{1(\tilde{\nu})}}{B_{2(\tilde{\nu})}} = \frac{\eta - (1+\eta)\gamma[\mathrm{H^+}]}{\sigma_{(\tilde{\nu})} + (1-\sigma_{(\tilde{\nu})})\gamma[\mathrm{H^+}]} \tag{15}$$

$$\gamma = \frac{k_3}{k_{\mathbf{TC}} - k_{\mathbf{Z}}} \tag{16}$$

$$\eta = \frac{[\mathbf{TC^*}]_0}{[\mathbf{Z^*}]_0} = \frac{k_2}{k_1} \tag{17}$$

$$\sigma_{(\tilde{\nu})} = \frac{\omega_{\mathbf{Z}(\tilde{\nu})}}{\omega_{\mathbf{TC}(\tilde{\nu})}} \tag{18}$$

Equation 12 predicts biexponential fluorescence decay with a pH-dependent lifetime τ_2 and an acidity-independent lifetime τ_1. Under selective excitation of **C** at band I and at acidities where **1** is completely protonated, this was indeed the behavior observed over a wide acidity range (Figures 3 and 4). The pH-independent lifetime τ_1 was found to have the same value as the monoexponential decay measured when **TC** is directly excited at absorption band II.

More light about the mechanism comes from the analysis of the amplitudes ratio as a function of the proton concentration (insets of Figures 3 and 4). The ratio B_1/B_2 goes from a negative value at high acidity to a positive value at $[\mathrm{H^+}] < 0.012$ mol dm^{-3} ($[\mathrm{H^+}] < 0.020$ mol dm^{-3} in D_2O). This behavior supports the existence of the $[\mathrm{H^+}]$-dependent excited-state protonation process **Z*** → **TC***.

To test the ability of the model to reproduce the experimental behavior, a global fit of eq 14 to the τ_2 fluorescence lifetime values and eq 15 to the B_1/B_2 amplitudes ratio data was performed in H_2O and D_2O, the fit yielding k_3, $k_{\mathbf{Z}}$, $k_{\mathbf{TC}}$, k_2/k_1, and $\sigma_{(\tilde{\nu})}$ (Table 2). The goodness of the fit (see the fitted functions represented as solid lines in Figures 3 and 4) supports the mechanism of Scheme 1. The values obtained for the protonation rate constant of **Z*** to give **TC*** (k_3) correspond, as expected, to a diffusion-controlled limit. The ratio k_2/k_1 provides information about a crucial aspect of the proposed mechanism, that is, the relative efficiency of the two competing phototautomerization processes undergone by **C***. Both in H_2O and D_2O, the ratio k_2/k_1 is close to unity, this meaning that deprotonation of **C*** to give **Z*** occurs at about the same rate than the water-assisted proton translocation of **C*** to yield **TC***.

TABLE 2: Rate Constants and Parameters Obtained from the Global Fit of Eq 14 to the τ_2 Fluorescence Lifetimes Values and Eq 15 to the B_1/B_2 Amplitudes Ratio Values at Various Emission Wavenumbers of Compound 1 in H_2O and D_2O at $\tilde{\nu}_{exc}$ = 31 250 cm^{-1} (Figures 3 and 4)

	H_2O		D_2O		
$k_3/10^9$ mol^{-1} dm^3 s^{-1}	10.37 ± 0.14		6.00 ± 0.10		
$k_Z/10^9$ s^{-1}	0.1906 ± 0.0019		0.1402 ± 0.0016		
$k_{TC}/10^9$ s^{-1}	0.475 ± 0.003		0.422 ± 0.003		
k_2/k_1	0.88 ± 0.02		1.00 ± 0.02		
$\sigma_{(\tilde{\nu})} = \omega_{Z(\tilde{\nu})}/\omega_{TC(\tilde{\nu})}$	0.232 ± 0.009 ($23\,810$ cm^{-1})	0.78 ± 0.03 ($21\,740$ cm^{-1})	0.112 ± 0.005 ($25\,000$ cm^{-1})	0.334 ± 0.015 ($23\,260$ cm^{-1})	0.96 ± 0.06 ($21\,280$ cm^{-1})

5. Principal Component Global Analysis of the Fluorescence Spectra of 1 under Selective Excitation of the Lactim Cation C at Absorption Band I: Fluorescence Spectrum of the Zwitterion Z*. To further confirm the proposed mechanism and obtain more information on the system, we applied principal component analysis to a series of 28 fluorescence spectra recorded in water (representative spectra plotted in Figure 2b) over the pH_c range 4.03−0.75 under excitation at band I (31 250 cm^{-1}). The analysis showed that three independent spectral components are needed to reproduce all the experimental spectra at the different acidities. Principal component global analysis with model functions derived from the proposed mechanism allowed us to obtain reliable estimations of the model parameters and the component spectra. According to our model, in the working acidity range the emissive species are **N***, **T***, **Z***, and **TC***, the last two formed through excitation of **C**, as it is the only cation absorbing significantly at the exciting wavenumber. Any fluorescence emission spectra **F** from the series can then be written as a linear combination of the spectra of the emissive species (eq 19).

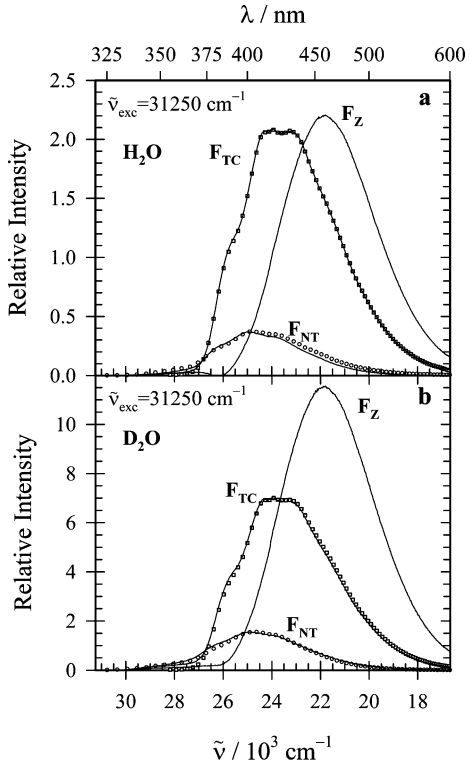

Figure 6. Results of the principal component global analysis of the fluorescence spectra of **1** in acid solutions recorded under excitation at band I (31 250 cm^{-1}) in (a) H_2O (series of 28 original spectra plotted in part in Figure 2b) and (b) D_2O. Shown here (solid lines) are the component spectra obtained, corresponding to the neutral forms **N*** and **T*** ($\mathbf{F_{NT}}$), the zwitterion **Z*** ($\mathbf{F_Z}$), and the lactam cation **TC*** ($\mathbf{F_{TC}}$). The experimental spectrum of **1** (○○○) obtained in neutral solutions of H_2O and D_2O at $\tilde{\nu}_{exc}$ = 31 250 cm^{-1} and the component spectrum corresponding to **TC*** (□□□) obtained from principal component global analysis of the fluorescence spectra recorded under excitation at band II ($\tilde{\nu}_{exc}$ = 28 570 cm^{-1}, see Figure 5 for H_2O) are also given here for comparison, normalized at the maximum intensity with those obtained in the present analysis. We used for these analyses the ratio $k_2/(k_1+k_2)$ = 0.468 in H_2O and 0.500 in D_2O provided from the time-resolved fluorescence results.

$$\mathbf{F} = c_N\mathbf{F_N} + c_T\mathbf{F_T} + c_Z\mathbf{F_Z} + c_{TC}\mathbf{F_{TC}} \tag{19}$$

In this equation, $\mathbf{F_N}$, $\mathbf{F_T}$, $\mathbf{F_Z}$, and $\mathbf{F_{TC}}$ represent the fluorescence spectra that would be obtained in the working conditions if each absorbed photon formed an excited molecule of the respective species, and the coefficients c represent the contribution of each spectrum to the experimental spectrum. As the acidity dependence of the steady-state concentrations of the neutral forms **N*** and **T*** is the same,[41] both species will always be in a fixed proportion at the exciting wavenumber at any acidity, and therefore eq 19 can be simplified to eq 20, where $c_{NT}\mathbf{F_{NT}} = c_N\mathbf{F_N} + c_T\mathbf{F_T}$ represents the combined fluorescence spectrum of the neutral forms in the working conditions.

$$\mathbf{F} = c_{NT}\mathbf{F_{NT}} + c_Z\mathbf{F_Z} + c_{TC}\mathbf{F_{TC}} \tag{20}$$

Taking into account the acidity dependence of the steady-state concentration of the respective excited species, eq 21 can be easily deduced from the mechanism (see the Supporting Information).

$$\mathbf{F} = c_{NT}\mathbf{F_{NT}} + c_2((1-\beta)\mathbf{F_Z} + \beta\mathbf{F_{TC}}) + c_3\mathbf{F_{TC}} \tag{21}$$

$$c_{NT} = \frac{K_a}{K_a + [H^+]} \tag{22}$$

$$c_2 = \frac{[H^+]}{(1+\alpha[H^+])(K_a + [H^+])} \tag{23}$$

$$c_3 = \frac{\alpha[H^+]^2}{(1+\alpha[H^+])(K_a + [H^+])} \tag{24}$$

$$\alpha = \frac{k_3}{k_Z} \tag{25}$$

$$\beta = \frac{k_2}{k_1 + k_2} \tag{26}$$

The three independent spectral components of the series of fluorescence spectra **F** at different acidities found by principal component analysis, $\mathbf{F_1}$, $\mathbf{F_2}$, and $\mathbf{F_3}$, are interpreted by our model as the three spectra whose coefficients have a different acidity dependence: (1) $\mathbf{F_1} = \mathbf{F_{NT}}$, the combined fluorescence spectrum of the neutral forms at the working excitation wavenumber, with coefficient c_{NT} representing the acidity dependence of the ground-state concentration of the neutral forms **N** and **T**; (2) $\mathbf{F_2} = (1-\beta)\mathbf{F_Z} + \beta\mathbf{F_{TC}}$, the combined spectrum of the zwitterion

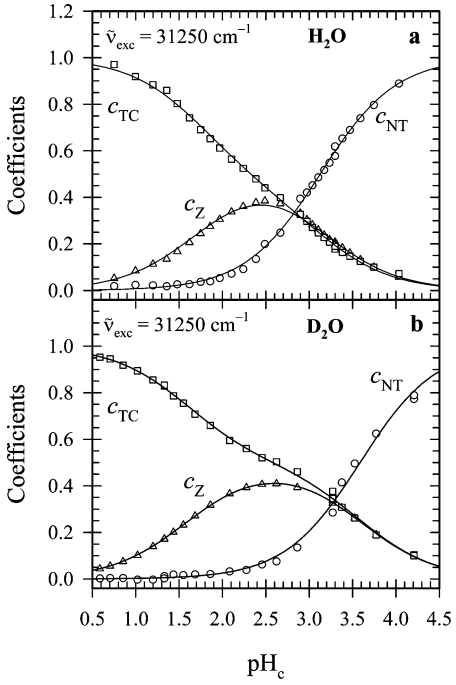

Figure 7. Principal component global analysis of the fluorescence spectra of **1** in acid solutions recorded under excitation at band I (31 250 cm^{-1}) in (a) H_2O (series of 28 original spectra plotted in part in Figure 2b) and (b) D_2O. Shown here are the coefficients (unfilled symbols) representing the pH-dependent contributions of the component spectra (displayed in Figure 6) of the neutral forms **N*** and **T*** (c_{NT}), the zwitterion **Z*** (c_Z), and the lactam cation **TC*** (c_{TC}). The solid lines represent the fit of the equations derived from the proposed model to these data. We used for these analyses the ratio $k_2/(k_1+k_2) = 0.468$ in H_2O and 0.500 in D_2O provided from the time-resolved fluorescence results.

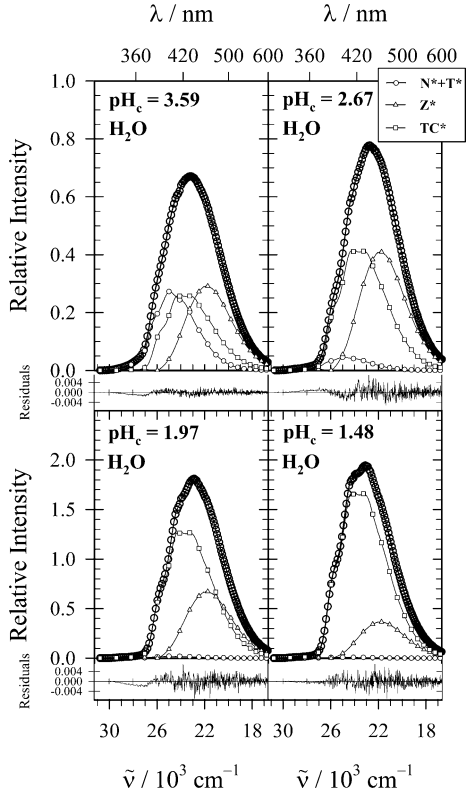

Figure 8. Experimental (solid line) and calculated (○○○) fluorescence spectra of **1** in aqueous solution at various acidities, together with the residual differences. The calculated spectra were obtained by principal component global analysis of a series of 28 spectra (plotted in part in Figure 2b) as linear combination of the component spectra $\mathbf{F_{NT}}$, $\mathbf{F_Z}$, and $\mathbf{F_{TC}}$, whose specific contributions at the working acidities are also shown. $\tilde{\nu}_{exc} = 31\,250$ cm^{-1}. [**1**] $= 3 \times 10^{-6}$ mol dm^{-3}.

Z and the lactam cation **TC**, with coefficient c_2 representing the direct formation of **Z*** and **TC*** from **C*** (rate constants k_1 and k_2); and (3) $\mathbf{F_3} = \mathbf{F_{TC}}$, the pure spectrum of the lactam cation, with coefficient c_3 representing the formation of **TC*** from **C*** through the zwitterion **Z***. The results of the principal component global analysis are shown in the Supporting Information.

From the global analysis described, the spectrum of the zwitterion **Z*** cannot be found unless the value of β is known (it can also not be directly measured, as it is always accompanied by that of **TC***). The time-resolved fluorescence data analysis described in the previous section provided the value of the quotient k_2/k_1 (Table 2), this leading to $\beta = 0.468$ in H_2O and 0.500 in D_2O. If principal component global analysis is again performed to the series of 28 emission spectra (part of them plotted in Figure 2b) with the set of eqs 20−24 and the above calculated value of β, the pure spectrum of **Z*** and the coefficients c_{NT}, $c_Z = c_2(1-\beta)$ and $c_{TC} = c_2\beta + c_3$, can be obtained. Principal component global analysis performed in this way yielded, in H_2O and D_2O, the component spectra shown in Figure 6 and the coefficients c_{NT}, c_Z, and c_{TC} of Figure 7. It is seen that as the pH$_c$ decreases, c_Z and c_{TC} initially increase and c_{NT} decreases due to ground-state protonation of the neutral forms to yield monocations **C** and **TC**. From pH$_c$ ∼2.5, c_Z decreases and c_{TC} further increases due to the protonation of **Z*** which yields **TC***. The quality of the fit can be appreciated in Figure 8, which shows the good agreement between the experimental fluorescence emission spectra of **1** in water at various acidities and the spectra calculated as linear combination of the contributions of $\mathbf{F_{NT}}$, $\mathbf{F_Z}$, and $\mathbf{F_{TC}}$ also shown in the figure. Similar results were obtained at all measured acidities in H_2O and D_2O.

A strong validation of the spectral decomposition performed comes from the comparison (Figure 6) of the component spectrum $\mathbf{F_{TC}}$ with the spectrum of the same species obtained under direct excitation of **TC** in absorption band II, showing perfect agreement between the two spectra. Also, the good coincidence of the spectra of the neutral forms **N*** and **T*** ($\mathbf{F_{NT}}$) with the experimental spectra measured in neutral solutions at the same excitation wavenumber (Figure 6) supports the validity of the interpretation of the component spectra.

The principal component global analysis performed yielded pK_a values in good agreement with those previously obtained (Table 1), and $k_3/k_Z = 57.3 \pm 1.2$ mol dm^{-3} in H_2O and 39.7 $\pm$ 1.0 mol dm^{-3} in D_2O. These values are in keeping with those obtained from the analysis of the fluorescence lifetimes shown in Table 2 ($k_3/k_Z = 54.4 \pm 0.9$ mol dm^{-3} in H_2O and 42.8 $\pm$ 0.9 mol dm^{-3} in D_2O), which brings support to the proposed model.

The good coincidence of the pK_a values obtained from the analysis of fluorescence and absorption spectra (Table 1) confirms that the neutral forms **N** and **T** do not protonate in the excited state and only disappear by ground-state protonation. This is an expected result, as the low proton concentration in the mild-acid to neutral media where **N** and **T** exist (pH > 2) makes the diffusion-controlled protonation process at least 10 times slower than the deactivation rate of species with ∼1 ns lifetime.[41]

TABLE 3: Ratio between the Fluorescence Intensity of TC* and Z* at Various Emission Wavenumbers, $F_{TC(\tilde{\nu})}/F_{Z(\tilde{\nu})}$, Obtained from Both Steady-State (SS)[a] and Time-Resolved (TR)[b] Fluorescence Data of 1 in H_2O and D_2O Acid Solutions

	H_2O		D_2O		
	23 810 cm^{-1}	21 740 cm^{-1}	25 000 cm^{-1}	23 260 cm^{-1}	21 280 cm^{-1}
$F_{TC(\tilde{\nu})}/F_{Z(\tilde{\nu})}$	1.79 (SS)	0.66 (SS)	2.85 (SS)	0.80 (SS)	0.35 (SS)
	1.73 (TR)	0.51 (TR)	2.97 (TR)	0.99 (TR)	0.35 (TR)

[a] Calculated from the pure fluorescence spectra of **TC*** and **Z*** obtained from principal component global analysis (Figure 6). [b] Obtained from eq 27 with the parameters provided by the time-resolved fluorescence data analysis (Table 2).

From the areas of the pure spectra $\mathbf{F_Z}$, $\mathbf{F_{TC}}$, and $\mathbf{F_{NT}}$, and knowing that in neutral aqueous solution under excitation at absorption band I the fluorescence quantum yield takes a value $\Phi = 0.074$,[41] the fluorescence quantum yields of **Z*** and **TC*** have been calculated (Table 1). As can be seen, the value of Φ_{TC} is in keeping with that obtained previously under excitation at band II. The spectral decomposition performed allowed to obtain in this way the fluorescence spectrum and quantum yield of the species **Z***, which cannot be independently measured.

The results of the principal component global analysis of the steady-state fluorescence can be further compared with the results obtained from the analysis of the time-resolved fluorescence data. The ratio between the fluorescence intensities of the pure spectra of **TC*** and **Z*** at any emission wavenumber $\{F_{TC(\tilde{\nu})}/F_{Z(\tilde{\nu})}\}$ may be written as

$$\frac{F_{TC(\tilde{\nu})}}{F_{Z(\tilde{\nu})}} = \left(\frac{\omega_{TC(\tilde{\nu})}}{\omega_{Z(\tilde{\nu})}}\right)\frac{k_2}{k_1}\frac{k_Z}{k_{TC}} \qquad (27)$$

The right-hand side of eq 27 can be calculated from the parameters provided by the analysis of the acidity dependence of the amplitudes ratio B_1/B_2 at the emission wavenumbers employed in the time-resolved fluorescence measurements (Table 2). The left-hand side of this equation can be directly evaluated at any $\tilde{\nu}$ from the fluorescence intensity of pure spectra of **TC*** and **Z*** (Figure 6) at that emission wavenumber. To compare both results, the evaluation of $\{F_{TC(\tilde{\nu})}/F_{Z(\tilde{\nu})}\}$ was performed at the emission wavenumbers employed in the time-resolved fluorescence measurements integrating an interval of 11 nm (spectral bandwidth of the emission monochromator for the time-resolved fluorescence data). The results of both calculations are compiled in Table 3. It is observed that for both H_2O and D_2O the values obtained from steady-state and time-resolved fluorescence data are very similar.

6. Hypothesis about Rotational Isomerism of the Lactim Cation. The lactim cation **C*** fluoresces strongly in acetonitrile,[43] but in water no fluorescence from this species could be detected. Our results show that this is due to the very fast disappearing of **C*** by two competing processes, the deprotonation of **C*** to give **Z*** (rate constant k_1) and the water-assisted phototautomerization **C*** → **TC*** (rate constant k_2). From the analysis of fluorescence lifetimes of **1** in acidic aqueous solution, we infer that the decay time of **C*** must be at least shorter than the time resolution of our single-photon counting equipment (0.1 ns), and therefore the rate constants k_1 and k_2 must be greater than 1×10^{10} s^{-1}. The existence of these ultrafast competing processes could be due to rotational isomerism involving the hydroxyl group of the lactim cation. We can envisage two types of rotameric structures, the syn rotamers $\mathbf{C^*_{syn}}$, with the OH group in close proximity to the pyridine N, and the anti rotamers $\mathbf{C^*_{anti}}$, with the OH group at a long distance from the N (see Scheme 2). The proximity of the OH group and the pyridine N in the syn rotamers will probably facilitate the proton translocation to give **TC***, while this process will be much slower for the anti rotamers due to the long distance OH···N. The proton transfer to the solvent will thus be the faster process for the anti rotamers, due to the enhanced acidity of the hydroxyl group in the excited state (Scheme 2).

SCHEME 2: Hypothesis about the Rotational Isomerism of the Lactim Cation and Its Influence on the Proton-Transfer Processes

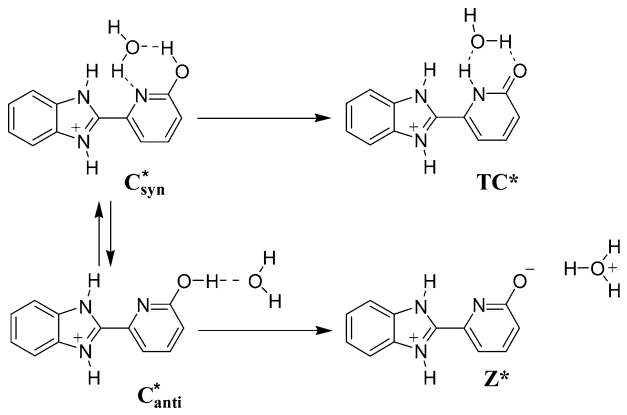

If the rate of internal rotation of the hydroxyl group (not free due to hydrogen bonding to solvent) is slower than the proton-transfer processes, no interconversion between the syn and anti rotamers will occur in the excited state. If the syn rotamer exclusively leads to **TC*** and the anti rotamer exclusively to **Z***, the rate constants ratio k_2/k_1 will depend only on the syn/anti concentration ratio in the ground state. If this is true, the values around 1 of k_2/k_1 in H_2O (0.88) and D_2O (1.00) will indicate the existence of approximately equal amounts of both rotamers in the ground state in both solvents. The type of spectral measurements performed does not allow us to prove this hypothesis.

Finally, we would like to comment on the protonation process **Z*** → **TC***. In Scheme 1, we propose a direct process, that is, protonation at the pyridine nitrogen. Nevertheless, it could also be possible that the protonation takes place at the oxygen atom. If the protonation leads to the syn rotamer $\mathbf{C^*_{syn}}$, it will immediately tautomerize to **TC***, according to the above hypothesis. This process would be indistinguishable by our measurements from the direct protonation at the pyridine nitrogen.

Conclusions

In this article we have studied the ground- and excited-state behavior of 2-(6′-hydroxy-2′-pyridyl)benzimidazolium in H_2O and D_2O. We have found that this compound shows in the ground state a tautomeric equilibrium between the lactim form **C**, protonated at the benzimidazole N(3), and its lactam tautomer **TC**, obtained by proton translocation from the hydroxyl group to the pyridine nitrogen. The tautomeric equilibrium constant $K = [\mathbf{TC}]/[\mathbf{C}]$ takes approximately the same value in H_2O (∼0.16) and D_2O (∼0.24). This feature is remarkably different from that observed in aprotic solvents such as acetonitrile, where

we have previously reported that **C** is the only species detected in the ground state.

We have also demonstrated that both cationic species follow very different excited-state deactivation patterns. Whilst the lactam tautomer **TC*** is deactivated via fluorescence emission and nonradiative pathways, the presence in the lactim cation **C*** of a hydroxyl group with enhanced acidity in the excited-state allows two competitive processes to occur: (a) water-assisted proton translocation to give **TC*** and (b) dissociation at the hydroxyl group to yield an emissive zwitterionic species **Z*,** which can further evolve to **TC*** by acid-catalyzed protonation. By combination of steady-state and time-resolved fluorescence data, together with principal component global analysis, we have been able to clarify the mechanistic details of both processes and the rate constants involved. The disappearance of **C*** in water is so fast that its fluorescence could not be detected. The competitive processes of proton transfer to the solvent **C*** → **Z*** and water-assisted proton translocation **C*** → **TC*** take place at about the same rate, both in H_2O and D_2O. We hypothesize that this fact is possibly due to the existence of rotational isomerism involving the hydroxyl group of the lactim cation. The syn rotamer, with the OH group in close proximity to the pyridine N, would lead easily to the lactam form with the assistance of a water molecule, while the anti rotamer, with the OH group at a long distance of the N, would faster dissociate, leading to the zwitterion **Z***. The fluorescence spectrum, lifetime, and quantum yield of the zwitterion (protonated at the benzimidazole N(3) and deprotonated at the hydroxyl group) have been determined.

Acknowledgment. We thank the Spanish Ministerio de Ciencia y Tecnología (Project BQU2001-3071), Ministerio de Educación y Ciencia (Project CTQ2004-07683-C02-01/BQU), and Xunta de Galicia (project PGIDIT02PXIC20907PN and Infraestructura Program) for financial support of this work.

Supporting Information Available: (a) Figures with the fluorescence decays of **1** in aqueous solution of $pH_c = 1.99$ at two excitation wavenumbers and fitted functions; (b) deduction of eqs 21−26; and (c) principal component global analysis of the fluorescence spectra of **1** under selective excitation of the lactim cation **C** at absorption band I. This material is available free of charge via the Internet at http://pubs.acs.org.

References and Notes

(1) Förster, T. *Naturwissenschaften* **1949**, *36*, 186.
(2) Weller, A. *Z. Elektrochem.* **1952**, *56*, 662.
(3) Weller, A. *Prog. React. Kinet.* **1961**, *1*, 187.
(4) Dermota, T. E.; Zhong, Q.; Castleman, A. W., Jr. *Chem. Rev.* **2004**, *104*, 1861.
(5) Waluk, J. *Acc. Chem. Res*. **2003**, *36*, 832.
(6) Tolbert, L. M.; Solntsev, K. M. *Acc. Chem. Res.* **2002**, *35*, 19.
(7) *Ultrafast Hydrogen Bonding Dynamics and Proton-Transfer Processes in the Condensed Phase;* Elsaesser, T., Bakker, H. J., Eds.; Kluwer Academic Publishers: Dordrecht, 2002.
(8) Chou, P. T. *J. Chin. Chem. Soc.* **2001**, *48*, 651.
(9) Waluk, J. In *Conformational Analysis of Molecules in Excited States*; Waluk, J., Ed.; Wiley-VCH: New York, 2000; Chapter 2, pp 57−111.
(10) Scheiner, S. *J. Phys. Chem A* **2000**, *104*, 5898.
(11) Ormson, S. M.; Brown, R. G. *Prog. React. Kinet.* **1994**, *19*, 45. Le Gourrierec, D.; Ormson, S. M.; Brown, R. G. *Prog. React. Kinet.* **1994**, *19*, 211.
(12) Arnaut, L. G.; Formosinho, S. J. *J. Photochem. Photobiol., A* **1993**, *75*, 1. Formosinho, S. J.; Arnaut, L. G. *J. Photochem. Photobiol., A* **1993**, *75*, 21.
(13) Kasha, M. *J. Chem. Soc., Faraday Trans. 2* **1986**, *82*, 2379.
(14) Lammers, S.; Meuwly, M. *Aust. J. Chem*. **2004**, *57*, 1223.
(15) Roscioli, J. R.; Pratt, D. W.; Smedarchina, Z.; Siebrand, W.; Fernández-Ramos, A. *J. Chem. Phys.* **2004**, *120*, 11351.
(16) Sato, H.; Hirata, F.; Sakaki, S. *J. Phys. Chem. A* **2004**, *108*, 2097.
(17) Freedman, H.; Nguyen, H. N.; Truong, T. N. *J. Phys. Chem. B* **2004**, *108*, 19043.
(18) Meuwly, M.; Müller, A.; Leutwyler, S. *Phys. Chem. Chem. Phys*. **2003**, *5*, 2663.
(19) Borst, D. R.; Roscioli, J. R.; Pratt, D. W.; Florio, G. M.; Zwier, T. S.; Müller, A.; Leutwyler, S. *Chem. Phys.* **2002**, *283*, 341.
(20) Matsuda, Y.; Ebata, T.; Mikami, N.; *J. Phys. Chem. A* **2001**, *105***,** 3475.
(21) Chou, P. T.; Wei, C. Y.; Hung, F. T.; *J. Phys. Chem. B* **1997**, *101*, 9119.
(22) Barone, V.; Adamo, C. *J. Phys. Chem*. **1995**, *99*, 15062.
(23) Ozeki, H.; Cockett, M. C. R.; Okuyama, K.; Takahashi, M.; Kimura, K.; *J. Phys. Chem.* **1995**, *99*, 8608.
(24) Barone, V.; Adamo, C. *J. Photochem. Photobiol., A* **1994**, *80*, 211.
(25) Hatherley, L. D.; Brown, R. D.; Godfrey, P. D.; Pierlot, A. P.; Caminati, W.; Damiani, D.; Melandri, S.; Favero, L. B. *J. Phys. Chem.* **1993**, *97*, 46.
(26) Sobolewski, A. *Chem. Phys. Lett*. **1993**, *211*, 293.
(27) Nowak, M. J.; Lapinski, L.; Fulara, J.; Les, A.; Adamowicz, L. *J. Phys. Chem.* **1992**, *96*, 1562.
(28) Nimlos, M. R.; Kelley, D. F.; Bernstein, E. R. *J. Phys. Chem.* **1989**, *93*, 643.
(29) Bensaude, O.; Chevrier, M.; Dubois, J. E. *J. Am. Chem. Soc.* **1979**, *101*, 2423.
(30) Bensaude, O.; Dreyfus, M.; Dodin, G.; Dubois, J. E. *J. Am Chem. Soc.* **1977**, *99*, 4438.
(31) Douhal, A.; Kim, S. K.; Zewail, A. *Nature* **1995**, *378*, 260. Goodman, M. F. *Nature* **1995**, *378*, 237.
(32) Taylor, C. A.; El-Bayoumi, M. A.; Kasha, M. *Proc. Natl. Acad. Sci. U.S.A.* **1969**, 63, 253.
(33) Guallar, V.; Douhal, A.; Moreno, M.; Lluch, J. M. *J. Phys. Chem. A* **1999**, *103*, 6251.
(34) Watson, J. H. D.; Crick, F. H. C. *Nature* **1953**, *171*, 737.
(35) Ogawa, A. K.; Abou-Zied, O. K.; Tsui, V.; Jimenez, R.; Case, D. A.; Romesberg, F. E. *J. Am. Chem. Soc*. **2000**, *122*, 9917.
(36) Wang, H.; Zhang, H.; Abou-Zied, O. K.; Yu, C.; Romesberg, F. E.; Glasbeek, M. *Chem. Phys. Lett.* **2003**, *367*, 599.
(37) Schultz, T.; Samoylova, E.; Radloff, W.; Hertel, I. V.; Sobolewski, A. L.; Domcke, W. *Science* **2004**, *306*, 1765.
(38) Sobolewski, A. L.; Domcke, W. *Phys. Chem. Chem. Phys.* **2004**, *6*, 2763.
(39) Díaz, N.; Suárez, D.; Sordo, T. L.; Méndez, R.; Villacorta, J. M. *Eur. J. Org. Chem.* **2003**, 4161.
(40) Yamada, M., Honma, I. *ChemPhysChem* **2004**, *5*, 724.
(41) Penedo, J. C.; Pérez Lustres, J. L.; García Lema, I.; Ríos Rodríguez, M. C.; Mosquera, M.; Rodríguez-Prieto, F. *J. Phys. Chem. A* **2004**, *108*, 6117.
(42) Ríos Rodriguez, M. C.; Mosquera, M.; Rodríguez-Prieto, F. *J. Phys. Chem. A* **2001**, *105*, 10249.
(43) Ríos Rodríguez, M. C.; Penedo, J. C.; Willemse, R. J.; Mosquera, M.; Rodríguez-Prieto, F. *J. Phys. Chem.* **1999**, *103*, 7236.
(44) Rodríguez-Prieto, F.; Ríos Rodriguez, M. C.; Mosquera González, M.; Ríos Fernández, M. A. *J. Phys. Chem.* **1994**, *98*, 8666.
(45) Ríos Rodriguez, M. C.; Rodríguez-Prieto, F.; Mosquera, M. *Phys. Chem. Chem. Phys.* **1999**, *1*, 253.
(46) Mosquera, M.; Penedo, J. C.; Ríos Rodríguez, M. C.; Rodríguez-Prieto, F. *J. Phys. Chem.* **1996**, *100*, 5398.
(47) Rodríguez Prieto, M. F.; Mosquera, M.; Novo, M. *J. Phys. Chem.* **1990**, *94*, 8536.
(48) Kondo, M. *Bull. Chem. Soc. Jpn.* **1978**, *51*, 3027.
(49) Brown, R. G.; Entwistle, N.; Hepworth, J. D.; Hodgson, K. W.; May, B. *J. Phys. Chem.* **1982**, *86*, 2418.
(50) Mosquera, M.; Ríos Rodríguez, M. C.; Rodríguez-Prieto, F. *J. Phys. Chem. A* **1997**, *101*, 2766.
(51) Jolliffe, I. T. *Principal Component Analysis*; Springer-Verlag: New York, 1986.
(52) Al-Soufi, W.; Novo, M.; Mosquera, M. *Appl. Spectrosc*. **2001**, *55*, 630.
(53) Novo, M.; Mosquera, M.; Rodríguez-Prieto, F. *Can. J. Chem*. **1992**, *70*, 823.
(54) Novo, M.; Mosquera, M.; Rodríguez-Prieto, F. *J. Phys. Chem.* **1995**, *99*, 14726.
(55) Reichardt, C. *Solvents and Solvent Effects in Organic Chemistry;* Wiley-VCH: Weinheim, 2003.